

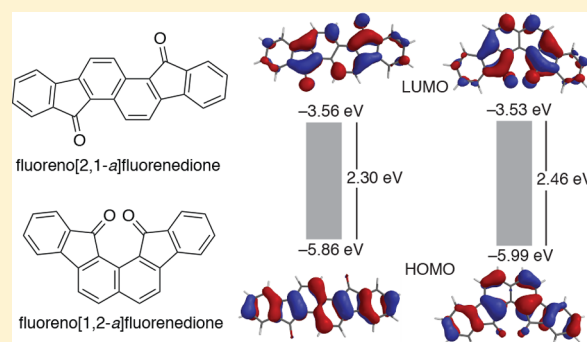
# Synthesis and Electronic Properties of Fluoreno[2,1-*a*]fluorenedione and Fluoreno[1,2-*a*]fluorenedione

Allison S. Hacker, Mauricio Pavano, James E. Wood, II, Chad E. Immoos, Hannah Hashimoto, Sam P. Genis, and Derik K. Frantz\*<sup>✉</sup>

Department of Chemistry and Biochemistry, California Polytechnic State University, 1 Grand Avenue, San Luis Obispo, California 93401, United States

**S** Supporting Information

**ABSTRACT:** The [2,1-*a*]- and [1,2-*a*]-isomers of fluorenofluorenedione have been synthesized via intramolecular Friedel–Crafts acylations. DFT calculations indicate that the [1,2-*a*]-isomer adopts a twisted, helical  $C_2$ -symmetric structure and that its protonated form is the thermodynamic product of the Friedel–Crafts acylation in hot sulfuric acid. Absorption spectroscopy and cyclic voltammetry measurements provide experimental estimations of frontier molecular orbital energy levels, which are reported and discussed.



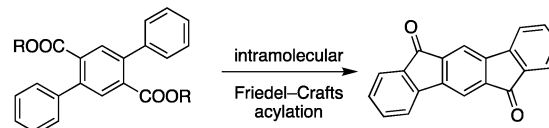
The synthesis of extended  $\pi$ -systems comprising polycyclic conjugated hydrocarbons (PCHs) permits fundamental investigations into concepts related to aromaticity and antiaromaticity<sup>1</sup> and enables applied research toward the development of functional organic materials.<sup>2</sup> In recent years, PCHs bearing a variety of structural arrangements have been featured in devices such as organic field-effect transistors<sup>3</sup> (OFETs), organic light-emitting diodes (OLEDs),<sup>4</sup> and organic photovoltaics (OPVs).<sup>5</sup> Strategies to access these extended PCHs often rely on cyclic ketones as synthetic intermediates. Ketones serve as direct precursors for  $\pi$ -extension via Wittig-type reactions, particularly Ramirez dibromoolefinations<sup>6</sup> and fulvene formation<sup>7</sup>, and have been employed in the synthesis of phenalenyl radicals<sup>8</sup> and bisphenalenyl systems. PCH-based diones are particularly useful as precursors to substituted  $\pi$ -extended molecules via addition of organometallic reagents followed by Sn-mediated reductive aromatization.<sup>10</sup> This methodology appears often in the chemical literature and has been featured in the synthesis of archetypal PCHs such as oligoacenes,<sup>11</sup> zethrenes,<sup>12</sup> and bisanthenes.<sup>13</sup>

Over the past decade, the groups of Haley<sup>14–16</sup> and Tobe<sup>17–19</sup> have generated a variety of Kekulé diradicaloid<sup>20</sup> indenofluorene (IF) isomers, all of which have been synthesized from IF-dione precursors.<sup>21</sup> Whereas isomers of IF possess benzenoid rings as cores, isomers of fluorenofluorene (FFs) contain central naphthalenoid groups. Three examples of FF, each deriving from dione intermediates, have been reported to date: Haley's closed-shell [4,3-*c*],<sup>22</sup> and [3,2-*b*]-isomers<sup>23</sup> and Tobe's substantially open-shell [2,3-*b*]-isomer.<sup>24</sup> Their usefulness as synthetic building blocks and as organic materials<sup>25</sup> motivates the synthesis and study of new PCH-based diones.

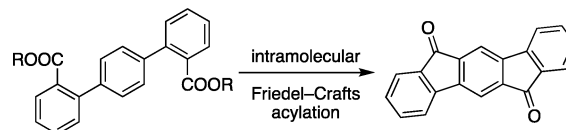
Synthesis of IF- and FF-based diones relies primarily on two strategies, which Haley categorizes as “inside-out” and “outside-in” (Scheme 1).<sup>14d</sup> Both methods employ intramolecular Friedel–Crafts acylation but differ in the locations of the acylium electrophiles. In the inside-out strategy, acylium ions

## Scheme 1. “Inside-Out” and “Outside-In” Strategies for IF-Dione Synthesis ([1,2-*b*]-Isomer Shown) and the “Outside-In” Approach to FF-Diones from Diones 1a and 1b

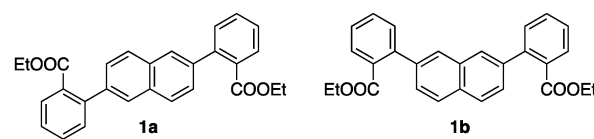
### “Inside-Out” synthetic strategy to indenofluorenediones



### “Outside-In” synthetic strategy to indenofluorenediones



### Precursors to FF-diones via “Outside-In” strategy in this study

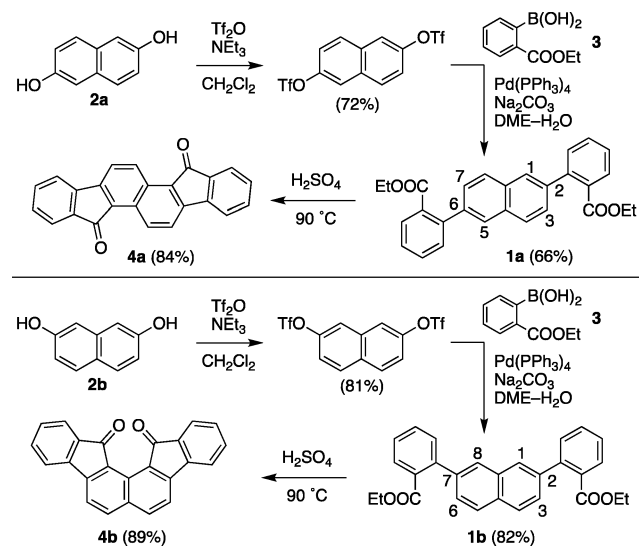


Received: October 24, 2017

located on the central aromatic ring add to the exterior benzene rings to form the polycyclic dione. Conversely, in the outside-in strategy, acylium ions located on the outer rings add to the central aromatic ring. Haley's syntheses of [4,3-*c*]- and [3,2-*b*]-FF-diones<sup>23</sup> and Tobe's synthesis of [2,3-*b*]-FF-dione<sup>24</sup> all make use of an inside-out strategy. Note that Haley used a Pd-catalyzed aryl–aryl cyclization developed by Scherf<sup>26</sup> in his original synthesis of [4,3-*c*]-FF-dione.<sup>22</sup> In the present study, we set out to synthesize and study fluorenofluorenediones via the outside-in strategy from diphenylnaphthalene-based diesters **1a** and **1b**.

Diesters **1a** and **1b** were synthesized from commercially available diols **2a** and **2b**, respectively (Scheme 2). Triflation

### Scheme 2. Synthesis of FF-Diones **4a** (Top) and **4b** (Bottom)



and subsequent Suzuki cross-coupling<sup>27</sup> reactions with 2-ethoxycarbonylbenzeneboronic acid (**3**) afforded **1a** and **1b** in gram quantities following a known procedure to diester **1a**.<sup>28</sup> Outside-in Friedel–Crafts acylation of **1a** generated dione **4a** (the [2,1-*a*]-isomer) in a high yield, a result that was unsurprising due to the higher nucleophilicity of naphthalene's 1- and 5-positions compared to its 3- and 7-positions. Although a ditheno analogue of **4a** has been recently described,<sup>29</sup> dione **4a** is reported only once in the chemical literature in a German patent from 1932. The patent describes the appearance of the compound in passing as “weinrot gefärbte, metallisch glänzende, schön ausgebildete Blätter” (red wine-colored, metallically shiny, beautifully shaped leaves).<sup>30</sup> We found that microcrystalline flakes and films of **4a** match the patent's description and that the fine powder form exhibits a lighter, bright-red color. The dione is sparingly soluble, a common characteristic for planar PCH-bearing diones.<sup>25</sup> Saturated, yet intrinsically highly dilute, solutions in CH<sub>2</sub>Cl<sub>2</sub> and acetone are faintly peach-colored, and slightly higher concentrations in refluxing toluene are yellow.

Remarkably, intramolecular Friedel–Crafts acylation of **1b** affords dione isomer **4b** (the [1,2-*a*]-isomer) exclusively in a high yield (Scheme 2, bottom). Compound **4b** is a bright-orange solid that, unlike compound **4a**, is moderately soluble as a bright-yellow solution in polar aprotic organic solvents. Computational models (B3LYP-6-31G\*) indicate that the ground state of molecule **4b** adopts a helical, C<sub>2</sub>-symmetric

structure to accommodate steric clashing, and likely electrostatic repulsion, of the two oxygen atoms (Figure 1a).

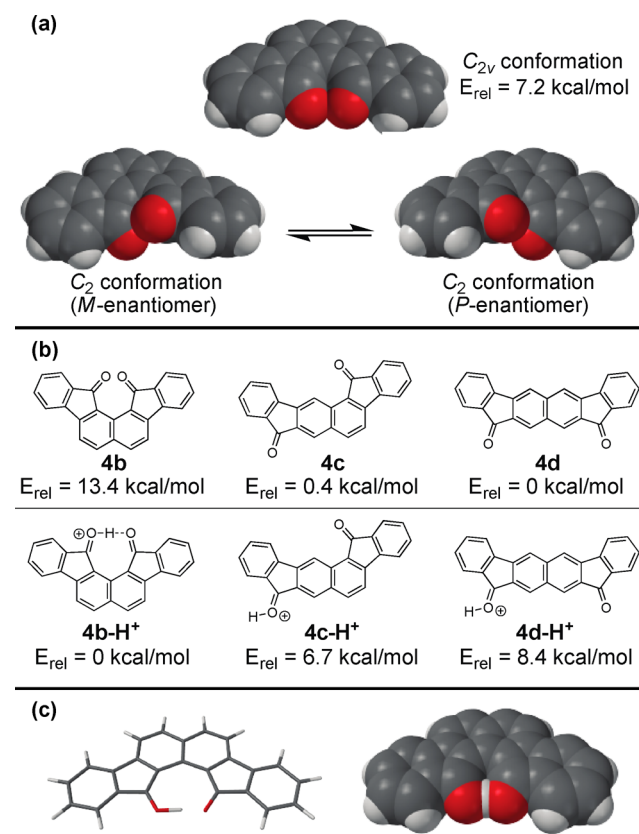


**Figure 1.** (a) Calculated structures of **4b** in C<sub>2</sub>- and C<sub>2v</sub>-symmetric conformations. (b) Calculated ground state energies for diones **4b**, **4c**, and **4d** and their protonated derivatives **4b-H<sup>+</sup>**, **4c-H<sup>+</sup>**, and **4d-H<sup>+</sup>**. Lowest-energy protonated isomers are shown. (c) Calculated structure of **4b-H<sup>+</sup>**, indicating the location of proton wedged between both ketones. All calculations were performed at the B3LYP-6-31G\* level of theory.

According to the calculations, the planar C<sub>2v</sub> structure lies 7.2 kcal/mol higher in energy, suggesting that enantiomeric, C<sub>2</sub>-symmetric structures of **4b** interconvert quickly by structural flipping at room temperature. We attribute dione **4b**'s high solubility relative to **4a** to its twisted molecular structure, which likely weakens intermolecular π-stacking interactions in the solid state,<sup>31</sup> and its substantial dipole moment, calculated to be 4.2 debye in the gas-phase ground state.

The calculations also predict that the ground state energy of dione **4b** is >13 kcal/mol higher in energy than those of the other two isomers (the [3,2-*a*]-isomer **4c** and the [2,3-*b*]-isomer **4d**) that could result from a rearrangement-free, intramolecular Friedel–Crafts acylation of **1b** (Figure 1b, top). The higher nucleophilicity of the 1- and 8-positions of the naphthalene core of **1b** could explain this result. Nucleophilicity is, however, a kinetic phenomenon, and the reaction in hot H<sub>2</sub>SO<sub>4</sub> is hardly under “kinetic control.” We propose that an intramolecular hydrogen-bonding interaction between the proximal oxygen atoms stabilizes the protonated structure of **4b** (Figure 1c) during the reaction. Calculations predict that the protonated [1,2-*a*]-isomer **4b-H<sup>+</sup>** lies 6.7 and 8.4 kcal/mol lower in energy than **4c-H<sup>+</sup>** and **4d-H<sup>+</sup>**, respectively (Figure 1b, bottom). This result suggests that **4b-H<sup>+</sup>** is indeed the

thermodynamic product of the reaction and affords **4b** after neutralization.

Absorption spectra of diones **4a** and **4b** reveal that both compounds exhibit weakly absorbing, low-energy  $S_0 \rightarrow S_1$  transitions in the visible region and strongly absorbing transitions in the UV range (Figure 2). As Haley and co-

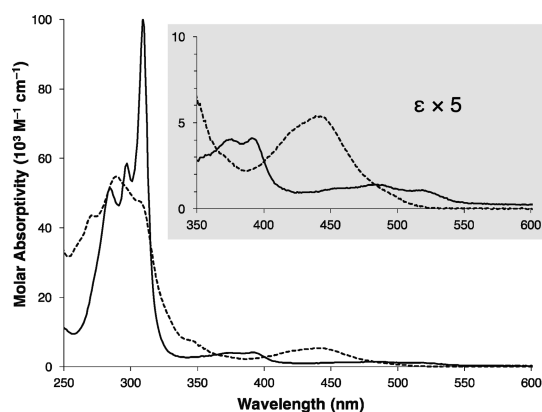


**Figure 2.** Absorption spectra of **4a** (solid line) and **4b** (dashed line) in  $\text{CH}_2\text{Cl}_2$ . Shaded area shows molar absorptivity ( $\epsilon$ ) multiplied by 5 over the range 350–600 nm.

workers point out,<sup>25</sup> the visible-range absorbances in IF-diones had been originally attributed to  $n \rightarrow \pi^*$  transitions;<sup>32</sup> TD-DFT calculations, however, predict that this absorbance arises from a  $\pi \rightarrow \pi^*$  transition. Given the structural and spectroscopic similarities between IF-diones and these FF-diones, it is likely that the visible transitions in **4a** and **4b** are also  $\pi \rightarrow \pi^*$  in nature. In the UV region, dione **4a** exhibits stronger and sharper absorptions with higher vibrational structure compared to dione **4b**. This result may arise from dione **4b**'s higher flexibility and reduced conjugation: the peripheral benzene rings in dione **4b** are nonconjugated, as they connect to the naphthalene core at the 2- and 7- positions in a *meta*-configuration.

The electrochemical properties of diones **4a** and **4b** were probed by cyclic voltammetry experiments (Figure 3). Both diones exhibit two reductions and no observable oxidations. Whereas **4a** exhibits two reversible reductions, the second reduction of **4b** is not completely reversible. The first reduction ( $E_{\text{red}1}$ ) occurs at nearly the same half-wave potential for both diones ( $E_{\text{red}1} = -1.43$  V for **4a** and  $-1.44$  V for **4b**). The second reduction ( $E_{\text{red}2}$ ) requires a substantially more negative potential for dione **4b** ( $-1.92$  V) compared to dione **4a** ( $-1.72$  V). The dianion of **4a** possesses a 1,8-naphthoquinodimethane core that can access both open- and closed-shell resonance forms (Scheme 3, top). The dianion of **4b**, however, is fundamentally diradical in nature and holds two oxygen atoms with a substantial negative charge in close proximity (Scheme 3, bottom). Negative charge repulsion likely increases the second reduction potential of **4b** compared to **4a**, and the diradical nature of **4b**<sup>2-</sup> renders it less stable than **4a**<sup>2-</sup>. The difference in potential between  $E_{\text{red}1}$  and  $E_{\text{red}2}$  in dione **4b** (0.48 V) closely matches that of indeno[2,1-*b*]fluorenedione (0.47 V),<sup>33</sup> an IF-dione whose dianion is also fundamentally diradical in nature.

Calculated structures of frontier molecular orbitals of **4a** and **4b**, and their experimentally determined energy levels, are presented in Figure 4. Based on onset potentials for their first reductions, LUMO energies for **4a** and **4b** are estimated to be  $-3.56$  eV and  $-3.53$  eV, respectively. Onset wavelengths for

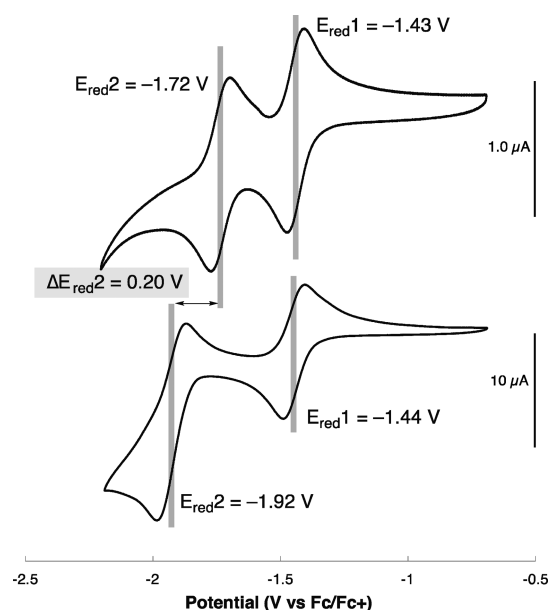
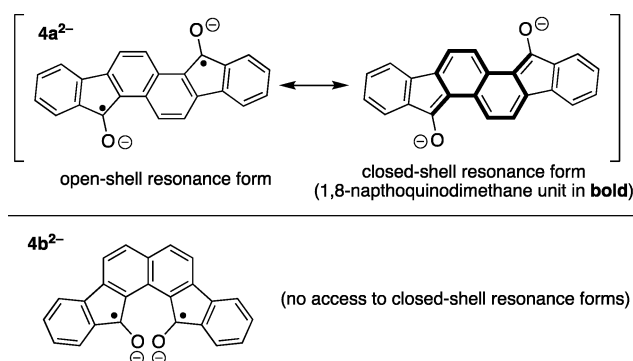


**Figure 3.** Cyclic voltammograms of dione **4a** (top) and dione **4b** (bottom). Measurements were performed in a 0.1 M solution of  $\text{Bu}_4\text{NPF}_6$  in  $\text{CH}_2\text{Cl}_2$  under  $\text{N}_2$  using a  $\text{Ag}/\text{AgNO}_3$  reference electrode, a Pt disk working electrode, and a Pt wire counter electrode. Dione **4a** is sparingly soluble and was measured as a saturated, yet dilute, solution. Dione **4b** was measured as a 1 mM solution.

### Scheme 3. Structures of Dianions of **4a** (Top) and **4b** (Bottom)



absorbance transitions estimate that the HOMO–LUMO energy gap ( $E_{\text{H-L}}$ ) of dione **4a** is 2.30 eV (540 nm) and that of dione **4b** is higher in energy at 2.46 eV (505 nm). Thus, HOMO energies lie at  $-5.86$  eV for **4a** and  $-5.99$  eV for **4b**.

In conclusion, we have used the outside-in Friedel–Crafts acylation strategy to generate the [2,1-*a*]- and [1,2-*a*]-isomers of fluorenofluorenedione selectively and in high yields from appropriately substituted diester precursors. Dione **4a** is red and sparingly soluble, and dione **4b** is orange and moderately soluble in polar aprotic organic solvents. Both molecules undergo two reductions in their cyclic voltammograms, and the potential and shape of the second reduction of **4b** reveals the instability of its dianion. The diones exhibit electronic absorptions in the visible and UV ranges. Current work is directed at employing these diones as synthetic building blocks for the generation of novel extended  $\pi$ -systems.

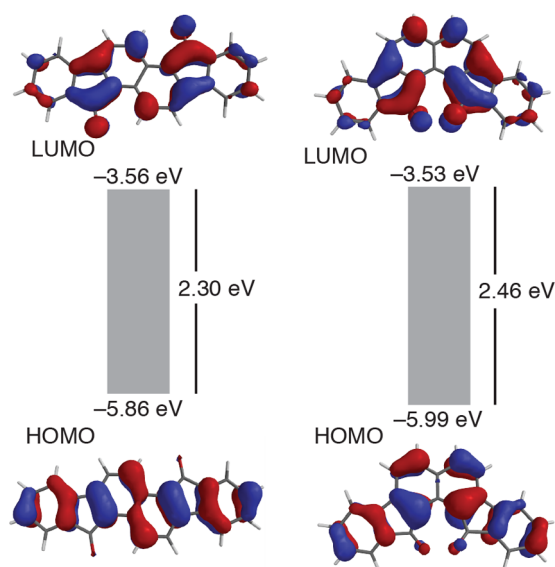


**Figure 4.** Experimentally determined HOMO and LUMO energies for diones **4a** (left) and **4b** (right) and their calculated (B3LYP-6-31G\*) orbital structures.

## EXPERIMENTAL SECTION

**General Information.** Synthetic procedures were performed open to air unless otherwise noted. Anhydrous THF was dried and stored over activated 3 Å molecular sieves. Other solvents and commercially available reagents were used as received without further purification. Analytical thin-layer chromatography was performed on Agela Technologies silica gel plates and visualized by 254 nm radiation. Column chromatography was performed with Sorbtech silica gel (60 Å, pH range 6.0–7.0). Melting ranges were recorded on a Vernier Melting Station apparatus. Nuclear magnetic resonance (NMR) spectra were recorded on a Bruker AVANCE II HD spectrometer at 400 MHz (100 MHz for  $^{13}\text{C}$ ). Chemical shifts for  $^1\text{H}$  NMR and  $^{13}\text{C}\{^1\text{H}\}$  NMR are reported in ppm ( $\delta$ ) relative to tetramethylsilane (0.00 ppm) or residual solvent (dichloromethane- $d_2$  5.33 ppm [for  $^1\text{H}$  NMR]). Multiplicity is indicated by one or more of the following: s (singlet); d (doublet); dd (doublet of doublets); td (triplet of doublets); dt (doublet of triplets). Broad signals are indicated with the abbreviation (br). Coupling constants ( $J$ ) are reported in hertz (Hz). Infrared spectra were recorded on a Thermo Scientific Nicolet iS5 Fourier transform infrared spectrometer (FTIR) using the attenuated total reflectance (ATR) technique on a diamond surface. Only peaks that are diagnostic of functional groups are reported. Percent transmittance of peaks is indicated relative to that of the strongest peak (normalized to 0%): s (0–33%); m (33–67%); w (67–100%). High-resolution mass spectra (HRMS) were measured at the Mass Spectrometry Laboratory in the School of Chemical Sciences, University of Illinois, Urbana–Champaign; ESI/Q-TOF measurements were performed on a Waters Q-TOF Ultima ESI instrument, and EI measurements were performed on a Waters 70-VSE instrument.

**Synthesis.** *2,6-Bis(trifluoromethylsulfonyloxy)naphthalene.* In a 250 mL, 1-neck round-bottom flask, a solution of 2,6-dihydroxynaphthalene (2.00 g, 12.5 mmol) in  $\text{CH}_2\text{Cl}_2$  (40 mL) and  $\text{Et}_3\text{N}$  (8 mL) was cooled to 0 °C over an ice bath. Triflic anhydride (5.0 mL, 30 mmol) was added steadily over 5 min while stirring. The dark reaction mixture was allowed to warm to room temperature and stirred for 20 h, after which  $\text{H}_2\text{O}$  (~10 mL) and  $\text{CH}_2\text{Cl}_2$  (~10 mL) were added to the mixture. The aqueous phase was extracted with  $\text{CH}_2\text{Cl}_2$ , and the combined organic phase was dried over  $\text{MgSO}_4$  and concentrated in vacuo. The dark brown oil was then purified by column chromatography (graduated from heptane to 8:2 heptane/ $\text{CH}_2\text{Cl}_2$ ), affording 2,6-bis(trifluoromethylsulfonyloxy)naphthalene as a colorless, crystalline solid (3.82 g, 72% yield). The obtained spectra

matched the literature spectra.<sup>28,34</sup>  $^1\text{H}$  NMR (400 MHz,  $\text{CDCl}_3$ ,  $\delta$ ): 7.98 (d, 2H,  $J$  = 8.9 Hz), 7.82 (d, 2H,  $J$  = 2.5 Hz), 7.49 (dd, 2H,  $J$  = 8.9, 2.4 Hz).

*2,6-Bis[2-(ethoxycarbonyl)phenyl]naphthalene (1a).* In a 250 mL, 3-neck round-bottom flask affixed with a condenser and two septa, 2,6-bis(trifluoromethylsulfonyloxy)naphthalene (3.00 g, 7.07 mmol),  $\text{Pd}(\text{PPh}_3)_4$  (0.654 g, 0.57 mmol), and *o*-ethoxycarbonylbenzoic acid (4.39 g, 22.6 mmol) were degassed with  $\text{N}_2$  (evacuation/refill). A solution of 20%  $\text{Na}_2\text{CO}_3$  (aq) (20 mL) and DME (50 mL) (separately degassed by the freeze–pump–thaw method) were added to the mixture, which was then stirred at 80 °C for 2.5 h. The resulting brown solution was allowed to cool to room temperature, and then  $\text{H}_2\text{O}$  (~10 mL) and EtOAc (~10 mL) were added to separate the phases. The aqueous phase was extracted with EtOAc, and the combined organic phase was dried over  $\text{MgSO}_4$  and concentrated in vacuo. The resulting brown oil was purified by column chromatography (silica,  $\text{CH}_2\text{Cl}_2$ /heptane 1:9). The fractions containing product were concentrated in vacuo, yielding a colorless solid (1.98 g, 66% yield). The obtained spectra matched the literature spectra.<sup>28</sup>  $^1\text{H}$  NMR (400 MHz,  $\text{CDCl}_3$ ,  $\delta$ ): 7.89 (dd, 2H,  $J$  = 7.8, 1.1 Hz), 7.86 (d, 2H,  $J$  = 8.4 Hz), 7.82 (d, 2H,  $J$  = 1.6 Hz), 7.58 (td, 2H,  $J$  = 7.5, 1.4 Hz), 7.51–7.42 (m, 6H), 4.08 (q, 4H,  $J$  = 7.1 Hz), 0.92 (t, 6H,  $J$  = 7.1 Hz).

*7H,14H-Dihydrofluoreno[2,1-*a*]fluorene-7,14-dione (4a).* Compound **1a** (965 mg, 2.22 mmol) was added to a 25 mL, 1-neck round-bottom flask. Concentrated sulfuric acid (8 mL) was then added, and the reaction was stirred at 90 °C for 35 min. The resulting dark green, acidic solution was neutralized with saturated, aqueous  $\text{NaHCO}_3$  in an ice bath, generating a dark purple-red precipitate. The precipitate was filtered and washed with  $\text{H}_2\text{O}$  and then washed with acetone to remove side products. After the acetone wash, the purple-red solid was triturated with hot toluene and allowed to cool to room temperature. Filtration afforded purple-red plates (623 mg, 84% yield).  $\text{Mp}$  >300 °C.  $^1\text{H}$  NMR (400 MHz,  $\text{CD}_2\text{Cl}_2$ ,  $\delta$ ): 9.09 (d, 2H,  $J$  = 8.3 Hz), 7.76 (d, 2H,  $J$  = 8.3 Hz), 7.53 (dt-like d, 2H,  $J$  = 7.4 Hz), 7.50 (dt-like d, 2H,  $J$  = 7.4 Hz), 7.44 (td, 2H,  $J$  = 7.4, 1.1 Hz), 7.24 (td, 2H,  $J$  = 7.4, 1.0 Hz).  $^{13}\text{C}$  NMR not measured due to sparing solubility of compound. HRMS (ESI/Q-TOF,  $m/z$ ): calcd for  $\text{C}_{24}\text{H}_{12}\text{O}_2$ , 332.0837; found, 332.0838. FTIR (neat,  $\text{cm}^{-1}$ ): selected absorptions 1696s, 1601m.

*2,7-Bis(trifluoromethylsulfonyloxy)naphthalene.* In a 500 mL round-bottom flask, a solution of 2,7-dihydroxynaphthalene (3.00 g, 18.8 mmol) in  $\text{CH}_2\text{Cl}_2$  (50 mL) and  $\text{Et}_3\text{N}$  (10 mL) was cooled to 0 °C. Triflic anhydride (7.6 mL, 45 mmol) was added steadily over 5 min while stirring. The dark reaction mixture was allowed to warm to room temperature and stirred for 3.5 h.  $\text{H}_2\text{O}$  (~10 mL) and  $\text{CH}_2\text{Cl}_2$  (~10 mL) were then added to the mixture, and the aqueous phase was extracted with  $\text{CH}_2\text{Cl}_2$ . The combined organic phase was dried over  $\text{MgSO}_4$  and concentrated in vacuo. The resulting dark brown oil was purified by column chromatography ( $\text{CH}_2\text{Cl}_2$ /heptane 2:8) to afford 2,7-bis(trifluoromethylsulfonyloxy)naphthalene as a colorless solid (6.50 g, 81% yield). The obtained spectra matched the literature spectra.<sup>34,35</sup>  $^1\text{H}$  NMR (400 MHz,  $\text{CDCl}_3$ ,  $\delta$ ): 8.00 (d, 2H,  $J$  = 9.1 Hz), 7.81 (d, 2H,  $J$  = 2.4 Hz), 7.48 (dd, 2H,  $J$  = 9.1, 2.4 Hz).

*2,7-Bis[2-(ethoxycarbonyl)phenyl]naphthalene (1b).* In a 250 mL, 3-neck round-bottom flask affixed with a condenser and two septa, 2,7-bis(trifluoromethylsulfonyloxy)naphthalene (3.00 g, 7.07 mmol),  $\text{Pd}(\text{PPh}_3)_4$  (656 mg, 0.57 mmol), and *o*-ethoxycarbonylbenzoic acid (4.39 g, 22.6 mmol) were degassed with  $\text{N}_2$  (evacuation/refill). A solution of 20%  $\text{Na}_2\text{CO}_3$  (aq) (20 mL) and DME (50 mL) (each separately degassed using the freeze–pump–thaw method with  $\text{N}_2$ ) were added to the reagent mixture via cannula. The resulting reaction mixture was stirred at 80 °C for 2.5 h. The resulting brown solution was cooled to rt, and then  $\text{H}_2\text{O}$  (~10 mL) and EtOAc (~10 mL) were added to separate the phases. The aqueous phase was extracted with EtOAc, and the combined organic phase was dried over  $\text{MgSO}_4$  and concentrated in vacuo. The resulting brown oil was purified by column chromatography ( $\text{CH}_2\text{Cl}_2$ /heptane 2:3), affording compound **1b** as a light yellow oil (2.45 g, 82% yield).  $^1\text{H}$  NMR (400 MHz,  $\text{CDCl}_3$ ,  $\delta$ ): 7.90–7.85 (m, 4H), 7.80 (br s, 2H), 7.57 (td, 2H,  $J$  = 7.52, 1.3 Hz), 7.49–7.43 (m, 6H), 4.08 (q, 4H,  $J$  = 7.1 Hz), 0.92 (t, 6H,  $J$  = 7.1 Hz).

$^{13}\text{C}$  NMR (100 MHz, acetone- $d_6$ ,  $\delta$ ): 168.8, 142.7, 140.2, 133.9, 132.6, 132.3, 132.0, 131.6, 130.4, 128.1, 128.0, 127.9, 127.8, 61.2, 14.0. HRMS (ESI/Q-TOF,  $m/z$ ) calcd for  $\text{C}_{28}\text{H}_{25}\text{O}_4$   $[\text{M} + \text{H}]^+$ , 425.1747; found, 425.1745.  $R_f$ : 0.48 (silica,  $\text{CH}_2\text{Cl}_2$ /heptane 1:1). FTIR (neat,  $\text{cm}^{-1}$ ): selected absorptions 2980w, 1709s, 1597m.

**13H,14H-Dihydrofluoreno[1,2-a]fluorene-13,14-dione (4b).** Compound **1b** (1.12 g, 2.65 mmol) was added to a 25 mL round-bottom flask. Concentrated sulfuric acid (8 mL) was then added, and the reaction was stirred at 90 °C for 40 min. The resulting dark mixture was added dropwise to a saturated solution of  $\text{NaHCO}_3$  to produce a bright orange precipitate, which was filtered, washed with  $\text{H}_2\text{O}$ , and allowed to dry, affording compound **4b** as a bright orange solid (780 mg, 89% yield). Mp 265–270 °C dec.  $^1\text{H}$  NMR (400 MHz,  $\text{CDCl}_3$ ,  $\delta$ ): 7.95 (d, 2H,  $J = 8.3$  Hz), 7.67 (d, 2H,  $J = 7.3$  Hz), 7.63 (d, 2H,  $J = 8.3$  Hz), 7.52 (d, 2H,  $J = 7.3$  Hz), 7.44 (td, 2H,  $J = 7.3, 1.1$  Hz), 7.32 (td, 2H,  $J = 7.3, 0.9$  Hz).  $^{13}\text{C}$  NMR (100 MHz,  $\text{CDCl}_3$ ,  $\delta$ ): 191.9, 149.4, 142.9, 137.2, 136.6, 135.5, 134.1, 130.5, 130.1, 124.80, 124.75, 120.7, 119.3. HRMS (EI,  $m/z$ ) calcd for  $\text{C}_{24}\text{H}_{12}\text{O}_2$ , 332.08373; found, 332.08345.  $R_f$ : 0.35 (silica,  $\text{CH}_2\text{Cl}_2$ /heptane 1:1). FTIR (neat,  $\text{cm}^{-1}$ ): selected absorptions 3041w, 1675s, 1605m.

**Absorption Spectra.** Absorption spectra were measured on an Agilent Technologies Cary Series UV–vis spectrophotometer using 10 mm quartz cuvettes in spectroscopic grade  $\text{CH}_2\text{Cl}_2$ . Molar absorptivities ( $\epsilon$ ) were measured according to the Beer–Lambert equation ( $\epsilon = Acl$ ). The reported spectra show the average  $\epsilon$  for each wavelength from three freshly prepared solutions of **4a** and **4b** ( $9.30 \times 10^{-6}$ ,  $1.23 \times 10^{-5}$ , and  $1.25 \times 10^{-5}$  for **4a**;  $1.17 \times 10^{-5}$ ,  $1.25 \times 10^{-5}$ ,  $1.36 \times 10^{-5}$  for **4b**).

**Cyclic Voltammetry.** Cyclic voltammetry (CV) measurements were performed under  $\text{N}_2$  on a CH Instruments potentiostat (Model 760B) using a  $\text{Ag}/\text{AgNO}_3$  reference electrode (containing a 0.01 M solution of  $\text{AgNO}_3$  in  $\text{CH}_3\text{CN}$ ), a Pt disk working electrode, and a Pt wire counter electrode. Measurements were performed at a sweep rate of 100 mV/s in dry, degassed  $\text{CH}_2\text{Cl}_2$  containing  $\text{Bu}_4\text{NPF}_6$  (0.1 M) as a supporting electrolyte. The ferrocene/ferrocenium ( $\text{Fc}/\text{Fc}^+$ ) reversible oxidation was used as an internal standard; Fc was added to the samples and measured directly after measurements of pure **4a** and **4b**. The LUMO energy levels of **4a** and **4b** were estimated using the following equation:

$$E_{\text{LUMO}}(\text{eV}) = -[E_{\text{onset}} - E_{\text{onset}}(\text{Fc}/\text{Fc}^+)] - 4.80 \text{ eV}$$

where  $E_{\text{onset}}$  is the onset potential for the first reductions of **4a** or **4b** and  $E_{\text{onset}}(\text{Fc}/\text{Fc}^+)$  is the onset potential for the oxidation of the  $\text{Fc}/\text{Fc}^+$ . The value  $-4.80$  eV is the HOMO energy of ferrocene compared to the vacuum level. The plots shown in Figure 3 are referenced against  $\text{Fc}/\text{Fc}^+$  (half-wave potential = 0 V). The value for  $E_{\text{onset}}(\text{Fc}/\text{Fc}^+)$  was determined to be  $-0.09$  V. The value for  $E_{\text{onset}}$  was determined to be 1.33 V for **4a** and 1.36 V for **4b**. Using the equation above, the LUMO energies for **4a** and **4b** were estimated to be  $-3.56$  eV and  $-3.53$  eV, respectively.

**Calculations.** Density functional calculations were performed using the B3LYP method in the 6-31G\* basis set. Calculations were performed using the Spartan 14 software package (Wavefunction, Inc. Irvine, CA, USA).<sup>36</sup>

## ASSOCIATED CONTENT

### Supporting Information

The Supporting Information is available free of charge on the ACS Publications website at DOI: 10.1021/acs.joc.7b02699.

NMR and IR spectra of compounds **1b**, **4a**, and **4b** and Cartesian coordinates of DFT-calculated structures (PDF)

## AUTHOR INFORMATION

### Corresponding Author

\*E-mail: dfrantz@calpoly.edu.

## ORCID

Derik K. Frantz: 0000-0002-7712-0479

## Notes

The authors declare no competing financial interest.

## ACKNOWLEDGMENTS

We acknowledge Cal Poly's Research, Scholarly, and Creative Activities (RSCA) Grant Program and the Frost Summer Research Program for financial support of this work. We thank Professor Michael M. Haley (University of Oregon) for helpful discussions. We thank the Mass Spectrometry Facility at the University of Illinois at Urbana–Champaign for measuring the mass spectra of new compounds.

## REFERENCES

- (1) Randić, M. *Chem. Rev.* **2003**, *103*, 3449–3606.
- (2) (a) Watson, M. D.; Fechtenkötter, A.; Müllen, K. *Chem. Rev.* **2001**, *101*, 1267–1300. (b) Wu, J.; Pisula, W.; Müllen, K. *Chem. Rev.* **2007**, *107*, 718–747.
- (3) (a) Zaumseil, J.; Sirringhaus, H. *Chem. Rev.* **2007**, *107*, 1296–1323. (b) Di, C.; Zhang, F.; Zhu, D. *Adv. Mater.* **2013**, *25*, 313–330.
- (4) Xiao, L.; Chen, Z.; Qu, B.; Luo, J.; Kong, S.; Gong, Q.; Kido, J. *Adv. Mater.* **2011**, *23*, 926–952.
- (5) Schlenker, C. W.; Thompson, M. E. *Top. Curr. Chem.* **2011**, *312*, 175–212.
- (6) Desai, N. B.; McKelvie, N.; Ramirez, F. J. *Am. Chem. Soc.* **1962**, *84*, 1745–1747.
- (7) (a) Mills, N. J. *Org. Chem.* **2013**, *78*, 4629–4641. (b) Usta, H.; Risko, C.; Wang, Z.; Huang, H.; Deliomeroğlu, M. K.; Zhukhovitskiy, A.; Facchetti, A.; Marks, T. J. *J. Am. Chem. Soc.* **2009**, *131*, 5586–5608. (c) Andrew, T. L.; Cox, J. R.; Swager, T. M. *Org. Lett.* **2010**, *12*, 5302–5305.
- (8) (a) Goto, K.; Kubo, T.; Yamamoto, K.; Nakasuji, K.; Sato, K.; Shiomi, D.; Takui, T.; Kubota, K.; Kobayashi, T.; Yakusi, K.; Ouyang, J. J. *Am. Chem. Soc.* **1999**, *121*, 1619–1620. (b) Uchida, K.; Ito, S.; Nakano, M.; Abe, M.; Kubo, T. *J. Am. Chem. Soc.* **2016**, *138*, 2399–2410.
- (9) Ohashi, K.; Kubo, T.; Masui, T.; Yamamoto, K.; Nakasuji, K.; Takui, T.; Kai, Y.; Murata, I. *J. Am. Chem. Soc.* **1998**, *120*, 2018–2027.
- (10) (a) Marshall, J. L.; Lehnerr, D.; Lindner, B. D.; Tykwinski, R. R. *ChemPlusChem* **2017**, *82*, 967–1001.
- (11) (a) Anthony, J. E. *Chem. Rev.* **2006**, *106*, 5028–5048. (b) Miao, Q. *Adv. Mater.* **2014**, *26*, 5541–5549.
- (12) (a) Sun, Z.; Zeng, Z.; Wu, J. *Acc. Chem. Res.* **2014**, *47*, 2582–2591. (b) Li, Y.; Heng, W.-K.; Lee, B. S.; Aratani, N.; Zafra, J. L.; Bao, N.; Lee, R.; Sung, Y. M.; Sun, Z.; Huang, K.-W.; Webster, R. D.; López Navarrete, J. T.; Kim, D.; Osuka, A.; Casado, J.; Ding, J.; Wu, J. *J. Am. Chem. Soc.* **2012**, *134*, 14913–14922. (c) Sun, Z.; Lee, S.; Park, K.; Zhu, X.; Zhang, W.; Zheng, B.; Hu, P.; Zeng, Z.; Das, S.; Li, Y.; Chi, C.; Li, R.; Huang, K.; Ding, J.; Kim, D.; Wu, J. *J. Am. Chem. Soc.* **2013**, *135*, 18229–18236.
- (13) (a) Li, J.; Zhang, K.; Zhang, X.; Huang, K.-W.; Chi, C.; Wu, J. *J. Org. Chem.* **2010**, *75*, 856–863. (b) Li, J.; Jiao, C.; Huang, K.-W.; Wu, J. *Chem. - Eur. J.* **2011**, *17*, 14672–14680.
- (14) For indeno[1,2-*b*]fluorene and derivatives, see: (a) Chase, D. T.; Rose, B. D.; McClintock, S. P.; Zakharov, L. N.; Haley, M. M. *Angew. Chem., Int. Ed.* **2011**, *50*, 1127–1130. (b) Chase, D. T.; Fix, A. G.; Rose, B. D.; Weber, C. D.; Nobusue, S.; Stockwell, C. E.; Zakharov, L. N.; Lonergan, M. C.; Haley, M. M. *Angew. Chem., Int. Ed.* **2011**, *50*, 11103–11106. (c) Chase, D. T.; Fix, A. G.; Kang, S. J.; Rose, B. T.; Weber, C. D.; Zhong, Y.; Zakharov, L. V.; Lonergan, M. C.; Nuckolls, C.; Haley, M. M. *J. Am. Chem. Soc.* **2012**, *134*, 10349–10352. (d) Frederickson, C. K.; Zakharov, L. N.; Haley, M. H. *J. Am. Chem. Soc.* **2016**, *138*, 16827–16838.
- (15) For indeno[2,1-*c*]fluorene, see: Fix, A. G.; Deal, P. E.; Vonnegut, C. L.; Rose, B. D.; Zakharov, L. N.; Haley, M. M. *Org. Lett.* **2013**, *15*, 1362–1365.

(16) For accounts of Haley's indenofluorenes and other quinoidal systems, see: (a) Frederickson, C. K.; Rose, B. D.; Haley, M. M. *Acc. Chem. Res.* **2017**, *50*, 977–987. (b) Haley, M. M. *Chem. Rec.* **2015**, *15*, 1140–1143.

(17) For indeno[2,1-*a*]fluorene, see: Shimizu, A.; Tobe, Y. *Angew. Chem., Int. Ed.* **2011**, *50*, 6906–6910.

(18) For indeno[2,1-*b*]fluorene, see: Shimizu, A.; Kishi, R.; Nakano, M.; Shiomi, D.; Sato, K.; Takui, T.; Hisaki, I.; Miyata, M.; Tobe, Y. *Angew. Chem., Int. Ed.* **2013**, *52*, 6076–6079.

(19) For a review/perspective of non-alternant non-benzenoid aromatic compounds, including indenofluorenes, see: Tobe, Y. *Chem. Rec.* **2015**, *15*, 86–96.

(20) Abe, M. *Chem. Rev.* **2013**, *113*, 7011–7088.

(21) Although not an indenofluorene, it is worth mentioning that Haley's extended diindenoanthracene was synthesized by another strategy using DDQ oxidation: Rudebusch, G. E.; Zafra, J. L.; Jorner, K.; Fukuda, K.; Marshall, J. L.; Arrechea-Marcos, I.; Espejo, G. L.; Ponce Ortiz, R.; Gomez-García, C. J.; Zakharov, L. N.; Nakano, M.; Ottosson, H.; Casado, J.; Haley, M. M. *Nat. Chem.* **2016**, *8*, 753–759.

(22) Rose, B. D.; Vonnegut, C. L.; Zakharov, L. N.; Haley, M. M. *Org. Lett.* **2012**, *14*, 2426–2429.

(23) Barker, J. E.; Frederickson, C. K.; Jones, M. H.; Zakharov, L. N.; Haley, M. M. *Org. Lett.* **2017**, *19*, 5312–5315.

(24) Miyoshi, H.; Miki, M.; Hirano, S.; Shimizu, A.; Kishi, R.; Fukuda, K.; Shiomi, D.; Sato, K.; Takui, T.; Hisaki, I.; Nakano, M.; Tobe, Y. *J. Org. Chem.* **2017**, *82*, 1380–1388.

(25) Rose, B. D.; Santa Maria, P. J.; Fix, A. G.; Vonnegut, C. L.; Zakharov, L. N.; Parkin, S. R.; Haley, M. M. *Beilstein J. Org. Chem.* **2014**, *10*, 2122–2130.

(26) Preis, E.; Scherf, U. *Macromol. Rapid Commun.* **2006**, *27*, 1105–1109.

(27) Miyaura, N.; Suzuki, A. *Chem. Rev.* **1995**, *95*, 2457–2483.

(28) Rao, R.; Desmecht, A.; Perepichka, D. F. *Chem. - Eur. J.* **2015**, *21*, 6193–6201.

(29) Ma, Y.; Zheng, Q.; Yin, Z.; Cai, D.; Chen, S.-C.; Tang, C. *Macromolecules* **2013**, *46*, 4813–4821.

(30) Kränzlein, G.; Wolfram, A.; Hausdörfer, E. Verfahren zur Darstellung von cyclischen Diketonen. German Patent 546226, March 10, 1932.

(31) (a) Smyth, N.; Van Engen, D.; Pascal, R. A., Jr. *J. Org. Chem.* **1990**, *55*, 1937–1940. (b) Shen, Y.; Chen, C.-F. *Chem. Rev.* **2012**, *112*, 1463–1535. (c) Fujikawa, T.; Segawa, Y.; Itami, K. *J. Am. Chem. Soc.* **2015**, *137*, 7763–7768.

(32) Rose, B. D.; Chase, D. T.; Weber, C. D.; Zakharov, L. N.; Lonergan, M.C.; Haley, M. M. *Org. Lett.* **2011**, *13*, 2106–2109.

(33) Romain, M.; Chevrier, M.; Bebiche, S.; Mohammed-Brahim, T.; Rault-Berthelot, J.; Jacques, E.; Poriel, C. *J. Mater. Chem. C* **2015**, *3*, 5742–5753.

(34) Frigoli, M.; Moustrou, C.; Samat, A.; Guglielmetti, R. *Eur. J. Org. Chem.* **2003**, *2003*, 2799–2812.

(35) Lombardo, C. M.; Welsh, S. J.; Strauss, S. J.; Dale, A. G.; Todd, A. K.; Nanjunda, R.; Wilson, W. D.; Neidle, S. *Bioorg. Med. Chem. Lett.* **2012**, *22*, 5984–5988.

(36) Shao, Y.; Molnar, L. F.; Jung, Y.; Kussmann, J.; Ochsenfeld, C.; Brown, S. T.; Gilbert, A. T. B.; Slipchenko, L. V.; Levchenko, S. V.; O'Neill, D. P.; DiStasio, R. A., Jr.; Lochan, R. C.; Wang, T.; Beran, G. T. O.; Besley, N. A.; Herbert, J. M.; Lin, C. Y.; Van Voorhis, T.; Chien, S. H.; Sodt, A.; Steele, R. P.; Rassolov, V. A.; Maslen, P. E.; Korambath, P. P.; Adamson, R. D.; Austin, B.; Baker, J.; Byrd, E. F. C.; Dachsel, H.; Doerksen, R. J.; Dreuw, A.; Dunietz, B. D.; Dutoi, A. D.; Furlani, T. R.; Gwaltney, S. R.; Heyden, A.; Hirata, S.; Hsu, C.-P.; Kedziora, G.; Khalliulin, R. Z.; Klunzinger, P.; Lee, A. M.; Lee, A. S.; Liang, W. Z.; Lotan, I.; Nair, N.; Peters, B.; Proynov, E. I.; Pieniazek, P. A.; Rhee, Y. M.; Ritchie, J.; Rosta, E.; Sherrill, C. D.; Simmonett, A. C.; Subotnik, J. E.; Woodcock, H. L., III; Zhang, W.; Bell, A. T.; Chakraborty, A. T.; Chipman, D. M.; Keil, F. J.; Warshel, A.; Hehre, W. J.; Schaefer, J. F.; Kong, J.; Krylov, A. I.; Gill, P. M. W.; Head-Gordon, M. *Phys. Chem. Chem. Phys.* **2006**, *8*, 3172–3191.